

Special Issue: Bio-based Packaging

Guest Editors: José M. Lagarón, Amparo López-Rubio, and María José Fabra
Institute of Agrochemistry and Food Technology of the Spanish Council for Scientific Research

EDITORIAL

Bio-based Packaging

J. M. Lagarón, A. López-Rubio and M. J. Fabra, *J. Appl. Polym. Sci.* 2015,
DOI: 10.1002/app.42971

REVIEWS

Active edible films: Current state and future trends

C. Mellinas, A. Valdés, M. Ramos, N. Burgos, M. D. C. Garrigós and A. Jiménez,
J. Appl. Polym. Sci. 2015, DOI: 10.1002/app.42631

Vegetal fiber-based biocomposites: Which stakes for food packaging applications?

M.-A. Berthet, H. Angellier-Coussy, V. Guillard and N. Gontard, *J. Appl. Polym. Sci.* 2015, DOI: 10.1002/app.42528

Enzymatic-assisted extraction and modification of lignocellulosic plant polysaccharides for packaging applications

A. Martínez-Abad, A. C. Ruthes and F. Vilaplana, *J. Appl. Polym. Sci.* 2015, DOI: 10.1002/app.42523

RESEARCH ARTICLES

Combining polyhydroxyalkanoates with nanokeratin to develop novel biopackaging structures

M. J. Fabra, P. Pardo, M. Martínez-Sanz, A. Lopez-Rubio and J. M. Lagarón, *J. Appl. Polym. Sci.* 2015, DOI: 10.1002/app.42695

Production of bacterial nanobiocomposites of polyhydroxyalkanoates derived from waste and bacterial nanocellulose by the electrospinning enabling melt compounding method

M. Martínez-Sanz, A. Lopez-Rubio, M. Villano, C. S. S. Oliveira, M. Majone, M. Reis and J. M. Lagarón, *J. Appl. Polym. Sci.* 2015,
DOI: 10.1002/app.42486

Bio-based multilayer barrier films by extrusion, dispersion coating and atomic layer deposition

J. Vartiainen, Y. Shen, T. Kaljunen, T. Malm, M. Vähä-Nissi, M. Putkonen and A. Harlin, *J. Appl. Polym. Sci.* 2015,
DOI: 10.1002/app.42260

Film blowing of PHBV blends and PHBV-based multilayers for the production of biodegradable packages

M. Cunha, B. Fernandes, J. A. Covas, A. A. Vicente and L. Hilliou, *J. Appl. Polym. Sci.* 2015, DOI: 10.1002/app.42165

On the use of tris(nonylphenyl) phosphite as a chain extender in melt-blended poly(hydroxybutyrate-co-hydroxyvalerate)/clay nanocomposites: Morphology, thermal stability, and mechanical properties

J. González-Ausejo, E. Sánchez-Safont, J. Gámez-Pérez and L. Cabedo, *J. Appl. Polym. Sci.* 2015, DOI: 10.1002/app.42390

Characterization of polyhydroxyalkanoate blends incorporating unpurified biosustainably produced poly(3-hydroxybutyrate-co-3-hydroxyvalerate)

A. Martínez-Abad, L. Cabedo, C. S. S. Oliveira, L. Hilliou, M. Reis and J. M. Lagarón, *J. Appl. Polym. Sci.* 2015,
DOI: 10.1002/app.42633

Modification of poly(3-hydroxybutyrate-co-3-hydroxyvalerate) properties by reactive blending with a monoterpene derivative

L. Pilon and C. Kelly, *J. Appl. Polym. Sci.* 2015, DOI: 10.1002/app.42588

Poly(3-hydroxybutyrate-co-3-hydroxyvalerate) films for food packaging: Physical-chemical and structural stability under food contact conditions

V. Chea, H. Angellier-Coussy, S. Peyron, D. Kemmer and N. Gontard, *J. Appl. Polym. Sci.* 2015, DOI: 10.1002/app.41850



Special Issue: Bio-based Packaging

Guest Editors: José M. Lagarón, Amparo López-Rubio, and María José Fabra
Institute of Agrochemistry and Food Technology of the Spanish Council for Scientific Research

Impact of fermentation residues on the thermal, structural, and rheological properties of polyhydroxy(butyrate-co-valerate) produced from cheese whey and olive oil mill wastewater
L. Hilliou, D. Machado, C. S. S. Oliveira, A. R. Gouveia, M. A. M. Reis, S. Campanari, M. Villano and M. Majone, *J. Appl. Polym. Sci.* 2015, DOI: [10.1002/app.42818](https://doi.org/10.1002/app.42818)

Synergistic effect of lactic acid oligomers and laminar graphene sheets on the barrier properties of polylactide nanocomposites obtained by the in situ polymerization pre-incorporation method

J. Ambrosio-Martín, A. López-Rubio, M. J. Fabra, M. A. López-Manchado, A. Sorrentino, G. Gorrasi and J. M. Lagarón, *J. Appl. Polym. Sci.* 2015, DOI: [10.1002/app.42661](https://doi.org/10.1002/app.42661)

Antibacterial poly(lactic acid) (PLA) films grafted with electrospun PLA/allyl isothiocyanate fibers for food packaging

H. H. Kara, F. Xiao, M. Sarker, T. Z. Jin, A. M. M. Sousa, C.-K. Liu, P. M. Tomasula and L. Liu, *J. Appl. Polym. Sci.* 2015, DOI: [10.1002/app.42475](https://doi.org/10.1002/app.42475)

Poly(L-lactide)/ZnO nanocomposites as efficient UV-shielding coatings for packaging applications

E. Lizundia, L. Ruiz-Rubio, J. L. Vilas and L. M. León, *J. Appl. Polym. Sci.* 2015, DOI: [10.1002/app.42426](https://doi.org/10.1002/app.42426)

Effect of electron beam irradiation on the properties of polylactic acid/montmorillonite nanocomposites for food packaging applications

M. Salvatore, A. Marra, D. Duraccio, S. Shayanfar, S. D. Pillai, S. Cimmino and C. Silvestre, *J. Appl. Polym. Sci.* 2015, DOI: [10.1002/app.42219](https://doi.org/10.1002/app.42219)

Preparation and characterization of linear and star-shaped poly L-lactide blends

M. B. Khajeheian and A. Rosling, *J. Appl. Polym. Sci.* 2015, DOI: [10.1002/app.42231](https://doi.org/10.1002/app.42231)

Mechanical properties of biodegradable polylactide/poly(ether-block-amide)/thermoplastic starch blends: Effect of the crosslinking of starch

L. Zhou, G. Zhao and W. Jiang, *J. Appl. Polym. Sci.* 2015, DOI: [10.1002/app.42297](https://doi.org/10.1002/app.42297)

Interaction and quantification of thymol in active PLA-based materials containing natural fibers

I. S. M. A. Tawakkal, M. J. Cran and S. W. Bigger, *J. Appl. Polym. Sci.* 2015, DOI: [10.1002/app.42160](https://doi.org/10.1002/app.42160)

Graphene-modified poly(lactic acid) for packaging: Material formulation, processing, and performance

M. Barletta, M. Puopolo, V. Tagliaferri and S. Vesco, *J. Appl. Polym. Sci.* 2015, DOI: [10.1002/app.42252](https://doi.org/10.1002/app.42252)

Edible films based on chia flour: Development and characterization

M. Dick, C. H. Pagno, T. M. H. Costa, A. Gomaa, M. Subirade, A. De O. Rios and S. H. Flóres, *J. Appl. Polym. Sci.* 2015, DOI: [10.1002/app.42455](https://doi.org/10.1002/app.42455)

Influence of citric acid on the properties and stability of starch-polycaprolactone based films

R. Ortega-Toro, S. Collazo-Bigliardi, P. Talens and A. Chiralt, *J. Appl. Polym. Sci.* 2015, DOI: [10.1002/app.42220](https://doi.org/10.1002/app.42220)

Bionanocomposites based on polysaccharides and fibrous clays for packaging applications

A. C. S. Alcântara, M. Darder, P. Aranda, A. Ayrál and E. Ruiz-Hitzky, *J. Appl. Polym. Sci.* 2015, DOI: [10.1002/app.42362](https://doi.org/10.1002/app.42362)

Hybrid carrageenan-based formulations for edible film preparation: Benchmarking with kappa carrageenan

F. D. S. Larotonda, M. D. Torres, M. P. Gonçalves, A. M. Sereno and L. Hilliou, *J. Appl. Polym. Sci.* 2015, DOI: [10.1002/app.42263](https://doi.org/10.1002/app.42263)



Special Issue: Bio-based Packaging

Guest Editors: José M. Lagarón, Amparo López-Rubio, and María José Fabra
Institute of Agrochemistry and Food Technology of the Spanish Council for Scientific Research

Structural and mechanical properties of clay nanocomposite foams based on cellulose for the food packaging industry

S. Ahmadzadeh, J. Keramat, A. Nasirpour, N. Hamdami, T. Behzad, L. Aranda, M. Vilasi and S. Desobry, *J. Appl. Polym. Sci.* 2015, DOI: [10.1002/app.42079](https://doi.org/10.1002/app.42079)

Mechanically strong nanocomposite films based on highly filled carboxymethyl cellulose with graphene oxide

M. El Achaby, N. El Miri, A. Snik, M. Zahouily, K. Abdelouahdi, A. Fihri, A. Barakat and A. Solhy, *J. Appl. Polym. Sci.* 2015, DOI: [10.1002/app.42356](https://doi.org/10.1002/app.42356)

Production and characterization of microfibrillated cellulose-reinforced thermoplastic starch composites

L. Lendvai, J. Karger-Kocsis, Á. Kmetty and S. X. Drakopoulos, *J. Appl. Polym. Sci.* 2015, DOI: [10.1002/app.42397](https://doi.org/10.1002/app.42397)

Development of bioplastics based on agricultural side-stream products: Film extrusion of *Crambe abyssinica*/wheat gluten blends for packaging purposes

H. Rasel, T. Johansson, M. Gällstedt, W. Newson, E. Johansson and M. Hedenqvist, *J. Appl. Polym. Sci.* 2015, DOI: [10.1002/app.42442](https://doi.org/10.1002/app.42442)

Influence of plasticizers on the mechanical and barrier properties of cast biopolymer films

V. Jost and C. Stramm, *J. Appl. Polym. Sci.* 2015, DOI: [10.1002/app.42513](https://doi.org/10.1002/app.42513)

The effect of oxidized ferulic acid on physicochemical properties of bitter vetch (*Vicia ervilia*) protein-based films

A. Arabestani, M. Kadivar, M. Shahedi, S. A. H. Goli and R. Porta, *J. Appl. Polym. Sci.* 2015, DOI: [10.1002/app.42894](https://doi.org/10.1002/app.42894)

Effect of hydrochloric acid on the properties of biodegradable packaging materials of carboxymethylcellulose/poly(vinyl alcohol) blends

M. D. H. Rashid, M. D. S. Rahaman, S. E. Kabir and M. A. Khan, *J. Appl. Polym. Sci.* 2015, DOI: [10.1002/app.42870](https://doi.org/10.1002/app.42870)



Modification of poly(3-hydroxybutyrate-co-3-hydroxyvalerate) properties by reactive blending with a monoterpene derivative

Laura Pilon,¹ Catherine Kelly²

¹UK Materials Technology Research Institute (A Pera Technology Ltd. Company), Pera Business Park, Nottingham Road, Melton Mowbray, Leicestershire LE13 0PB, United Kingdom

²School of Metallurgy and Materials, University of Birmingham, Birmingham B15 2TT, United Kingdom

Correspondence to: L. Pilon (E-mail: L.Pilon@peratechnology.com)

ABSTRACT: A one-step reactive blending approach is reported for modification of the thermal and mechanical properties of poly(3-hydroxybutyrate-co-3-hydroxyvalerate). A free-radical initiated reaction of the monoterpene derivative, linalool, was carried out with PHBV in the melt. This processing led to a reduction in the material melt temperature and increase in the tensile strength and elongation at break. Reduced embrittlement over time was also evident in the reactive blended materials in an ambient temperature ageing study, suggestive of reduced secondary crystallization. The nature of the structural changes within the materials could not be fully elucidated, but evidence pointed to free radical cross-linking, mediated by the linalool, as a major component of the changes.

© 2015 Wiley Periodicals, Inc. *J. Appl. Polym. Sci.* **2016**, *133*, 42588.

KEYWORDS: biopolymers and renewable polymers; cross-linking; crystallization; mechanical properties; thermoplastics

Received 24 February 2015; accepted 3 June 2015

DOI: 10.1002/app.42588

INTRODUCTION

With increasing pressure on fossil-fuel-based raw materials and limitations on space for/increases in cost of disposal of plastic articles via landfill, biosourced and biodegradable polymers are set to become progressively more important. A wide range of applications and articles such as packaging, disposable cups and cutlery, waste bags, and medical devices such as sutures, tissue scaffolds, and controlled release implants can all derive advantages from the use of biodegradable materials.^{1–4} Particularly of interest for packaging are materials that can be composted alongside food and garden waste in domestic or municipal processes to create useful products for agriculture and horticulture. Of all the biodegradable polymers, polyhydroxyalkanoates (PHAs) are of particular interest due to their combination of sustainable sourcing and biodegradability thereby addressing both resource scarcity and waste issues. PHAs are also relatively stable to hydrolysis and have significantly improved barrier properties over PLA and starch-based materials (suggesting potential applications in modified atmosphere packaging).^{5,6} However, these materials are at a relatively early stage of development and commercialization due to some remaining challenges that need to be overcome.

PHAs are typically prepared using a microbial synthesis method from a variety of renewable feedstocks such as sugars and fatty

acids.⁷ Poly(3-hydroxybutyrate) (P3HB) is the most widely available variant, along with some products based on copolymers with poly(3-hydroxyvalerate) (P3HV), poly(3-hydroxyhexanoate) (P3HH), and poly(4-hydroxybutyrate) (P4HB). The preparation of copolymers allows modification of properties such as crystallinity, flexibility, elongation, and melt flow rate for various processing routes and applications. A number of technical barriers to expansion of commercial applications of PHAs exist however. First, the processing window of these materials is narrow. The melting point of P3HB is around 165°C, but it starts to degrade above 180°C as evidenced by molecular weight reduction of extruded materials.⁵ Second, the processing of these materials is challenging due to low melt viscosity and slow crystallization from the melt. These factors cause difficulties in processes that require high melt strength (such as blown film extrusion) and reduce processing rates relative to conventional polymers due to the extended crystallization times that are required to reduce tackiness of extruded strands prior to pelletization and of injection molded parts prior to removal. Third, the high crystallinity of P3HB and tendency to produce large, microcrack-containing spherulites leads to brittleness of the material. Finally, the slow crystallization continues at ambient temperature over prolonged periods of time, causing further embrittlement of the material.

Additional Supporting Information may be found in the online version of this article.

© 2015 Wiley Periodicals, Inc.

A number of approaches have been attempted for property modification of PHAs,⁵ including preparation of copolymers,⁸ inclusion of nucleating agents during extrusion compounding,⁹ blending with other polymeric ingredients,^{9–13} and reactive extrusion.^{14,15} Of particular interest in this instance was reactive extrusion for incorporation of side groups and/or light cross-linking. This approach was expected to improve flexibility by reduction of crystallinity, and also limit chain mobility to prevent long-term embrittlement caused by secondary crystallization.

Reactive extrusion has long been used for property modification of olefins and this subject was extensively reviewed by Moad in 1999.¹⁶ The review focused on free radical grafting reactions of unsaturated monomers, particularly maleic anhydride, due to the tendency of this monomer not to undergo homopolymerization. Hence, such monomers are typically attached to the polymer backbone as discrete molecular units rather than as oligomeric chains. Reactive extrusion has since been extended successfully to biodegradable polyesters, also using the maleic anhydride route. For example, Hassouna *et al.* reported the two-step reactive extrusion of polylactide (PLA) with maleic anhydride in the first step and with citrate,¹⁷ or poly(ethylene glycol) in the second step.¹⁸ Inhibition of plasticizer grafting and improved retention of mechanical properties were achieved. Reports of PHB modification by similar routes include the free-radical cross-linking of PHBV using dicumyl peroxide (DCP) as the initiator¹⁵ and peroxy-initiated maleation of PHB in a reactive extrusion process reported by Misra *et al.* in 2004.¹⁴ A key disadvantage of the maleic anhydride route to reactive extrusion is its two-step nature: with the low decomposition temperature of PHAs, it is important to minimize the number of thermal processing steps that are carried out on the materials.

Aims

This investigation aimed to improve the mechanical properties of PHBV, particularly with regard to reducing long-term embrittlement. A free radical modification approach was chosen, but it was decided to avoid the two-step maleic anhydride-based process discussed in the introduction to minimize the known thermal decomposition of PHBV at the required processing temperatures and also to avoid the use of respiratory sensitizers (maleic anhydride). Unsaturated natural products were the focus for our one-step process; linalool (a component of lavender and other essential oils) was chosen as the modification agent due to its low toxicity, process compatibility, and wide availability. The disadvantage of using linalool as the modifier in a single-step reaction is the presence of multiple free-radical reactive sites and therefore the potential for the formation of a complex series of products.

EXPERIMENTAL

Materials

Poly(3-hydroxybutyrate-co-3-hydroxyvalerate) (PHBV, Tianan Enmat Y1000P) was obtained from Helian Polymers and dried under reduced pressure for 1 h at 80°C prior to processing. Linalool (97%) and dicumyl peroxide (DCP, 98%) were obtained from Sigma-Aldrich and used as received. Solvents (chromatog-

raphy grade) were obtained from Sigma-Aldrich or Fisher Scientific and used as received.

Processing

Linalool (4.5 wt %), DCP (0–4 wt %, 0–1 equivalents of radicals with respect to linalool), and PHBV (91.5–95.5 wt %), with a total batch size of 50 g were mixed in a Haake PolyLab QC twin-screw compounder with a set temperature of 160°C and a screw speed of 100 rpm. Melt temperature (thermocouple positioned in the mixer wall) and torque profiles were recorded over the 15 min residence time, before the mixed product was collected and allowed to cool. Film samples were prepared by pressing at 180°C and up to 5 tons pressure between a pair of release films. Samples were stored at 2–8°C prior to testing.

Aging

Pressed film samples were aged at ambient temperature (18–20°C) and normal atmosphere, with the exclusion of light. Samples were withdrawn for tensile testing on a weekly basis for the first month and monthly thereafter for a total of 3 months.

Characterization

Gas chromatography (GC) was carried out using a HP 5890 Series II GC equipped with an Rtx-5 (30 m × 0.25 mm × 0.25 μm) column and FID detector. The oven temperature was ramped to 200°C (1. 50°C for 5 min; 2. Ramp to 200°C at 15°C min⁻¹; 3. 200°C for 5 min) and the detector was held at 250°C. A 0.5 μL injection was analyzed using a split injection mode (split ratio 33 : 1) and a carrier gas (He) flow of 1.5 mL min⁻¹. Samples were dissolved in chloroform using sonication, then diluted with methanol to a known concentration (1 : 4 chloroform : methanol) and filtered to 0.45 μm prior to injection to remove the precipitated polymer. Calibration standards of 100, 200, and 500 ppm linalool were prepared using the same solvent mixture.

IR spectroscopy was carried out using a Shimadzu FTIR-8400S equipped with an ATR accessory in the range 500–4000 cm⁻¹.

¹H NMR spectroscopy was performed at University of Leicester, Department of Chemistry using a 500 MHz Bruker spectrometer, standard ¹H experiment parameters, and CDCl₃ as the solvent.

Gel permeation chromatography (GPC) was carried out using an Agilent PL220 GPC equipped with 2 × PLGel mixed B columns and a refractive index (RI) detector. Chloroform (stabilized with amylene) was used as the eluent at a flow rate of 1.0 mL min⁻¹ and with a column oven temperature of 30°C. Calibration was performed using Agilent Easival polystyrene standards. Samples were prepared at approximately 2 mg mL⁻¹ in the eluent and filtered to 0.45 μm prior to injection.

Differential scanning calorimetry (DSC) was performed using a Perkin Elmer DSC 8000, under nitrogen flow at 20 mL min⁻¹ and calibrated at the appropriate heating rates using Indium and Zinc standards. All samples were conditioned to standardize their thermal history by heating above the melt point. For glass transition temperature (*T*_g) measurements, the sample was then cooled to -40°C at a rate of 20°C min⁻¹ and subsequently heated to 60°C at 100°C min⁻¹. *T*_g was calculated in the

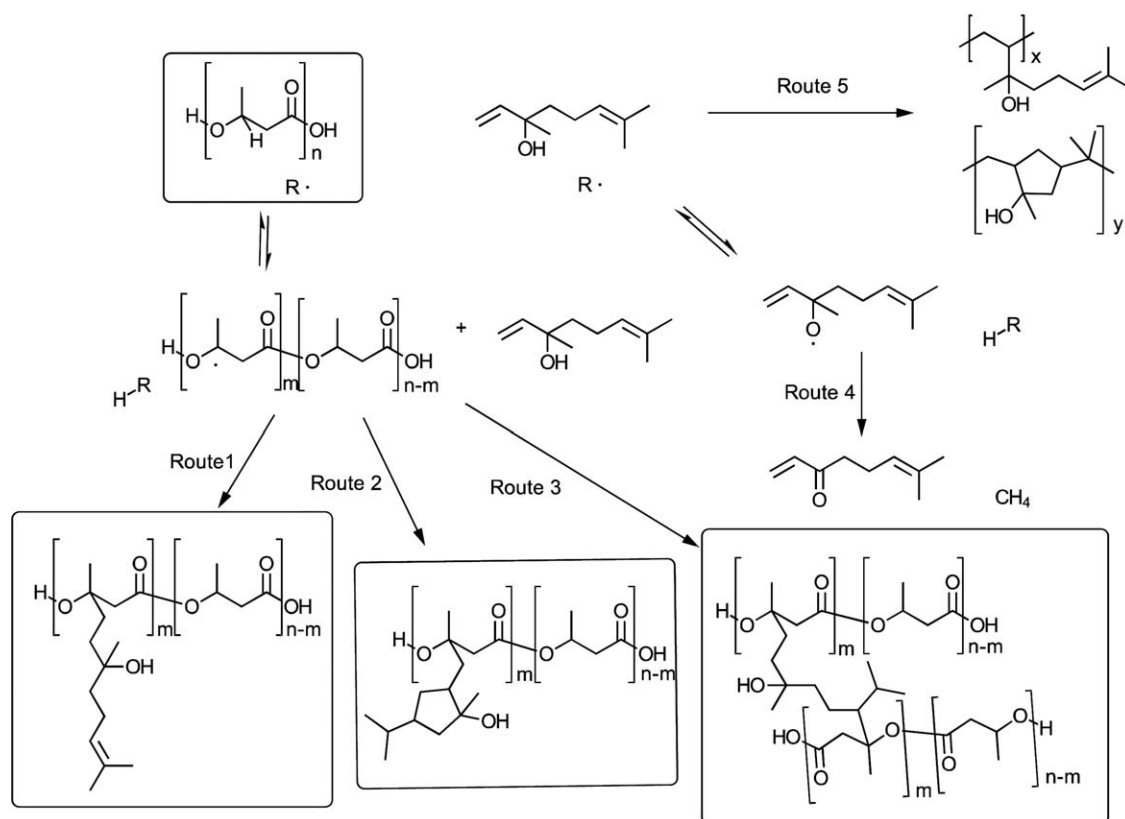


Figure 1. A range of potential modes of reaction for linalool with PHBV under melt-phase conditions with free-radical initiation. Only the 3-hydroxybutyrate (not the 3-hydroxyvalerate) repeat units of PHBV are shown for clarity. Potential products arising from various grafting/cross-linking reactions with linalool are highlighted in boxes.

instrument software as the “half C_p ” value. Crystallization and melting temperatures (T_c and T_m) were recorded as the peak of the exotherm/endothrm on $20^\circ\text{C min}^{-1}$ cooling/heating cycles respectively. Sample size was 2.5–3.5 mg.

Thermogravimetric analysis (TGA) was performed using a Perkin Elmer Pyris 1 TGA under nitrogen atmosphere. Mass loss was recorded between 40 and 350°C at a heating rate of $10^\circ\text{C min}^{-1}$.

Dynamic mechanical analysis (DMA) was carried out at University of Birmingham using a Netzsch DMA 242 cooled with liquid nitrogen. Strips ($50 \times 11 \times 0.9$ mm) were cut from hot-pressed sheets of (reactive) blended PHBV and analyzed using the three-point bend geometry. Measurements were taken at a frequency of 1 Hz as the temperature was increased from -50 to 100°C at a rate of 2°C min^{-1} .

Time zero tensile testing was performed at Pera Technology using a Testometric FS300CT equipped with a 50 kg load cell. Small dog bone samples with a gauge length of 35 mm and a width of 5 mm were cut from polymer film sheets using a standard cutter and tested to failure at a cross-head speed of 2 mm min^{-1} . At least 5 replicates were tested for each sample. Further tensile testing for aging studies was performed at University of Birmingham on 13×75 mm dog bone samples (3 replicates for each sample) using an Instron 5566 equipped with a 1 N load cell at the same rate of 2 mm min^{-1} .

RESULTS AND DISCUSSION

Potential Reaction Routes

A range of potential modes of reaction for linalool were considered (Figure 1) and are listed as follows. Additional degradation reactions such as chain scission and elimination of crotonic acid are not listed. These reaction routes are referenced later in the discussion, relating to particular evidence gathered during characterization of the products.

1. Maleic anhydride grafting of polyolefins, PLA, and PHAs is reported to proceed via hydrogen abstraction at tertiary carbon centers followed by free radical addition to the maleic anhydride double bond.^{14–18} Therefore, the first reaction to consider is that of only a single double bond of the linalool (incorporation as a side group).
2. Concerted reaction of both double bonds in a cyclization reaction (incorporation as a cyclic side group).¹⁹
3. Separate reaction of both double bonds (cross-linking, branching, or large loop formation).
4. Proton abstraction from linalool hydroxyl and subsequent rearrangement. The resulting α,β -unsaturated ketone product still retains both double bond functionalities and therefore could still be attached to the polymer backbone by any of processes 1–3.
5. Direct polymerization of linalool.²⁰
6. Direct cross-linking of PHBV chains by radical combination (not shown in Figure 1).

Table I. Summary of Mix Composition and Mix Monitoring

Sample no	Target linalool content (wt %)	DCP content (wt %)	Maximum temperature reached (°C)	Maximum torque reached (Nm)	Actual "free" linalool content (wt % by GC)
1	0	0	178	22	N/A
2	4.5	0	178	13	1.8
3	4.5	1	170	10	0.7
4	4.5	2	178	10	0.3
5	4.5	4	187	16	0.1

The set temperature of the mixer was 160°C as described in the section titled "Experimental".

7. Transesterification of PHBV ester group with linalool hydroxyl group (not shown in Figure 1). Could be catalyzed by carboxylic acid end groups and/or crotonic acid degradation products.

Material Processing and Chemical Characterization

A summary of the samples prepared for this investigation is shown in Table I. These materials included 2 control samples; PHBV alone and PHBV blended with linalool in the absence of the DCP initiator, in addition to the reactive blended materials of interest. The residence time of the ingredients in the mixer was chosen as 5 half lives ($t_{1/2}$) for DCP at the set temperature to ensure effectively complete initiator decomposition during the timescale of the experiment.¹⁶ DSC analysis of DCP showed a broad exotherm with onset around 130°C and peak at 178°C, attributable to the decomposition. Figure 2 shows an overlay of the temperature and torque profiles for selected mixes. The temperature profiles for samples 4 and 5 show clear step changes in melt temperature that were absent in the profiles of mixes without DCP. These temperature increases were therefore attributed to exothermic reactions taking place in the melt: the lower temperature step coinciding approximately with the DSC exotherm for DCP (subject to errors arising from differences in heating rate). These temperature increases were also coincident with increases in mixer torque resulting from increased melt viscosity. Higher levels of DCP incorporation were not

attempted due to the likelihood of hazardous larger temperature rises and significant PHBV decomposition.

After preparation, the quantity of "free" linalool remaining in the materials was evaluated using GC analysis. Due to the volatility of linalool (boiling point $\sim 200^\circ\text{C}$) at the processing temperature of 160–170°C, less than 50% of the originally added linalool was incorporated into the PHBV in the absence of DCP. On increasing the quantity of DCP included in the mixture, the amount of free (i.e., unreacted) linalool decreased further, to as low as 0.1 wt % at the maximum level of DCP inclusion. These results suggested first that the linalool was sufficiently thermally stable at the processing temperature and second that the reaction of the linalool had occurred in the presence of the DCP.

The analysis of chemical changes in the samples was expected to be challenging due to low grafting efficiencies typically achieved in these types of processes: values of the order of 0.5–1.0% are typically reported for maleic anhydride using an acid/base titration method.^{21,22} The complicated combination of expected chemical structures arising from the modification process reported herein and therefore the lack of an obvious chemical analysis method for the attached linalool meant that grafting efficiency could not be determined. Despite these issues, some qualitative chemical analysis was carried out using ^1H NMR and FTIR spectroscopy to attempt to infer the type of reaction product.

Analysis of the ^1H NMR spectra (see Supporting Information, Figures S1–S3) was complicated by incomplete dissolution of the samples in CDCl_3 , even after warming, which led to peak broadening, poor resolution, and variable integrals. Peaks for the DCP decomposition by-product, acetophenone, could be observed around 7–8 ppm for samples 3–5, consistent with the expected homolytic fission of the peroxide bond and subsequent rearrangement of the 2-phenylisopropoxy radical with the elimination of a methyl radical as the primary initiating species. Peaks due to the linalool vinyl groups (and alkyl groups in their vicinity) could clearly be seen in the region of 5–6 ppm and 2 ppm for sample 2 (PHBV/linalool blend), but not sample 5 (prepared with 4% DCP). In sample 5, new, broad peaks were observed in the region of 1–2 ppm that could not be attributed to PHBV peaks. The positioning of the larger of these peaks at 1.7 ppm was consistent with the position of a linalool CH_2 group, although its higher intensity than expected would

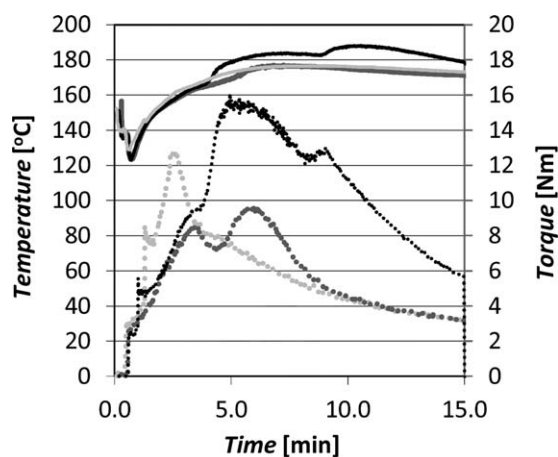


Figure 2. Temperature (solid lines) and torque (dotted lines) overlays for mixes 2 (pale grey), 4 (dark grey), and 5 (black), showing coincidence of torque increases with temperature increases.

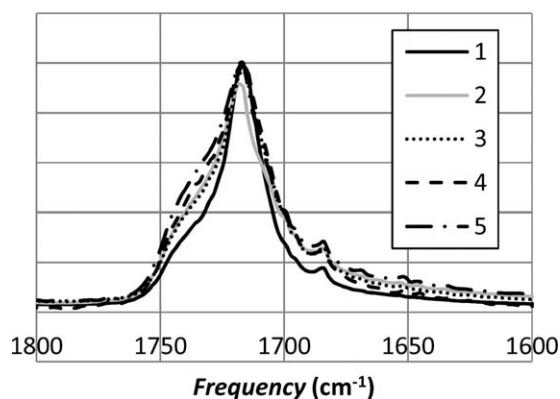


Figure 3. Carbonyl region of the FTIR spectra of samples 1–5 showing a shift in the peak position with simple linalool blending and broadening/shoulder development as DCP concentration was increased in the reactive blending experiments. 1, solid black (control); 2, solid grey (0% DCP); 3, dotted black (1% DCP); 4, dashed black (1% DCP); 5, dot/dashed black (4% DCP).

suggest overlap with additional groups from a saturated linalool reaction product. Due to the broadening of the spectrum, it could not be determined whether this product was most likely to be cyclic or linear (or a mixture). The lack of additional vinyl peaks suggests that the rearrangement of linalool to the α,β -unsaturated ketone product of reaction route 4 (Figure 1) is unlikely, but could not be completely ruled out. On the basis of the chemical evidence presented, it is considered that reaction routes 2 and 3 are the most likely of those proposed, but insufficient detail was evident in the ^1H NMR spectrum to distinguish between them. Previous literature also only showed minor changes to NMR spectra of PHBV on reactive processing.¹⁵

Few obvious differences could be observed in the FTIR spectra of samples 1–5, in particular, peaks due to linalool were expected to overlap PHBV peaks and would therefore not be detected at the low levels expected. This result was expected on the basis of literature reports for reactive extrusion of PLA with maleic anhydride, which showed only limited changes to the FTIR.^{17,18} However, closer inspection of the carbonyl peak (Figure 3) did show broadening and shoulder development at 1740 cm^{-1} that increased with DCP concentration. This new shoulder could not be attributed to the presence of the acetophenone by-product of the reaction, whose carbonyl peak appears at $\sim 1680\text{ cm}^{-1}$ or to carboxylic acid carbonyls (such as crotonic acid, a known degradation product of PHBV) arising from chain scission processes since these also appear at lower frequency than ester carbonyls.²¹ Fei *et al.* suggest that the appearance of the shoulder may arise from an increase in the amorphous content of the PHBV, which would be expected from these products.²²

GPC analysis was additionally carried out to determine if changes in molecular weight could be detected that would assist further elucidation of the mode of reaction and resulting chemical structures present. In common with the NMR analysis, difficulties were experienced in achieving complete dissolution for certain samples. Although poor solubility is common for PHBV due to its high crystallinity, samples 1 and 2 dissolved readily in

chloroform with heating while samples 3 and 4 appeared to dissolve, but were difficult to filter and sample 5 had insoluble fragments. Due to the poor solubility and necessary filtration of samples, chromatograms do not show the entire molecular weight distribution, but only the soluble fraction. Results of the GPC analysis are shown in Table II (see Supporting Information, Figure S4, for chromatograms). It was difficult to distinguish a clear trend in M_n , but M_p of the soluble fraction was found to decrease as DCP concentration was increased. Additionally, all samples containing DCP had higher polydispersities than the blends without DCP. The apparent decrease in M_p for samples 4 and 5 is attributed to an artifact of discarding the insoluble portion of the sample and is consistent with cross-linking of the higher molecular weight portion of the sample as exploited in the synthesis of highly branched acrylic polymers.^{23,24} An additional explanation for the change in solubility could be a change in chemical structure (addition of new side groups via routes 1 and 2), but due to the expected low grafting efficiency, this explanation is not thought to be likely. There were no new peaks in the chromatograms that could be attributed to free poly/oligolinalool (i.e., not grafted to PHBV), but this should not be treated as evidence of the absence of poly/oligolinalool since such peaks could be coincident with the PHBV peak. Transesterification of PHBV esters with linalool hydroxyl groups (route 7) was eliminated as a potential reaction since no molecular weight reduction or peak broadening was noted between samples 1 and 2 (PHBV processed alone and PHBV blended with linalool).

Thermal Characterization

Thermal analysis of the materials was carried out using TGA, DSC, and DMA (Table III, Figures 4, 5, and Supporting Information Figures S5, and S6). Linalool was found to have a slight protective effect on PHBV with regard to its thermal decomposition as measured by TGA: an enhancement in thermal stability of approximately 20°C was achieved by incorporation of linalool in the blend. This enhancement of thermal stability appeared to be limited to materials containing free linalool and might therefore be related to the linalool unsaturation acting as a “sink” for thermally generated free radicals: T_d sample 2 (no DCP) $>$ T_d samples 3 and 4 (low DCP) $>$ T_d samples 1 and 5 (no linalool and high DCP respectively).

A summary of DSC and DMA data is shown in Table III and DSC scans are shown in Figure 4 (melt/crystallization) and

Table II. GPC Results as a Function of Initiator Concentration for the Soluble Portions of Samples 1–5. Samples 3 and 4 Initially Appeared Soluble, But were Difficult to Filter and Sample 5 Contained an Obvious Insoluble Fraction

Sample	[DCP] (wt %)	M_p	M_n	M_w/M_n
1	0	148,700	78,900	2.40
2	0	151,800	80,700	2.43
3	1	103,100	61,700	2.50
4	2	80,800	80,800	3.49
5	4	51,700	27,300	2.82

Table III. Summary of Thermal Analysis Data for (Reactive) Blended PHBV Samples

Sample	[DCP] (%)	T_g (°C)		T_m (°C)		ΔH_m (total) ($J g^{-1}$)	T_c (°C)	ΔH_c ($J g^{-1}$)
		DSC	DMA	1	2			
1	0	2.1	19	168	None	83.0	113	-75.8
2	0	4.4 ^a	12	168	None	75.8	116	-68.3
3	1	2.4	9	161	Shoulder	71.8	110	-65.7
4	2	4.6	9	153	162	69.2	103	-64.5
5	4	6.0	10	147	156	64.0	103	-58.5

^aUnclear transition, so large experimental error in this value assumed.

Supporting Information (Supporting Information Figure S5, glass transition). DMA traces are shown in Figure 5 (tan δ) and Supporting Information (Figure S6, E'). T_m and T_c of sample 1 (control) by DSC were consistent with those reported for Enmat Y1000P PHBV by Corre *et al.*⁶ No significant changes in T_m were caused by simple blending of PHBV with linalool (2). However, the T_g was observed to decrease by DMA, as would be expected if linalool acts as a plasticizer. In addition, the T_c for sample 2 by DSC increased relative to the control indicating enhancement of crystallization. This effect would be expected for a plasticized material since reduced melt viscosity would allow polymer chains to achieve crystalline conformations more rapidly.

Crystallization and melting seemed more affected than T_g by reactive blending of PHBV with linalool. The incorporation of increasing levels of DCP initiator to the mixture was found to result in decreasing T_c (Figure 4), indicating inhibition of crystallization by the reactive blending process. Values of T_m (and their decrease with DCP content) were consistent with those reported by Fei *et al.* for DCP-cross-linked PHBV, but our values of T_c were higher than previously reported for similar levels

of DCP, as was our relative decrease in T_c .¹⁵ This difference in T_c values is probably related to differences in the DSC protocols used, but the difference in the relative decrease in T_c should not be method-dependent and therefore could potentially be influenced by the mediating effect of the linalool on the cross-linking/grafting reaction. A PHBV modification protocol that reduces T_m , but limits the effect on T_c has potential advantages for industrial processing since slow crystallization rates for PHBV increase the time in-mold (for example) so it would be disadvantageous to reduce crystallization rates significantly. However, further investigation is needed on the crystallization kinetics of these materials to confirm whether this is indeed the case.

A further change in the melt behavior of these materials was a change from a single melt peak for the simple PHBV/linalool blend to a dual melt peak for the reactive blended PHBV/linalool. This dual melt peak was consistent with literature reports of recrystallization processes occurring during the melt transition for maleated PHB.²⁵ Chen *et al.* also showed a decrease in T_m of the initial melting as the degree of grafting increased: in this study, similarities and differences to this behavior were

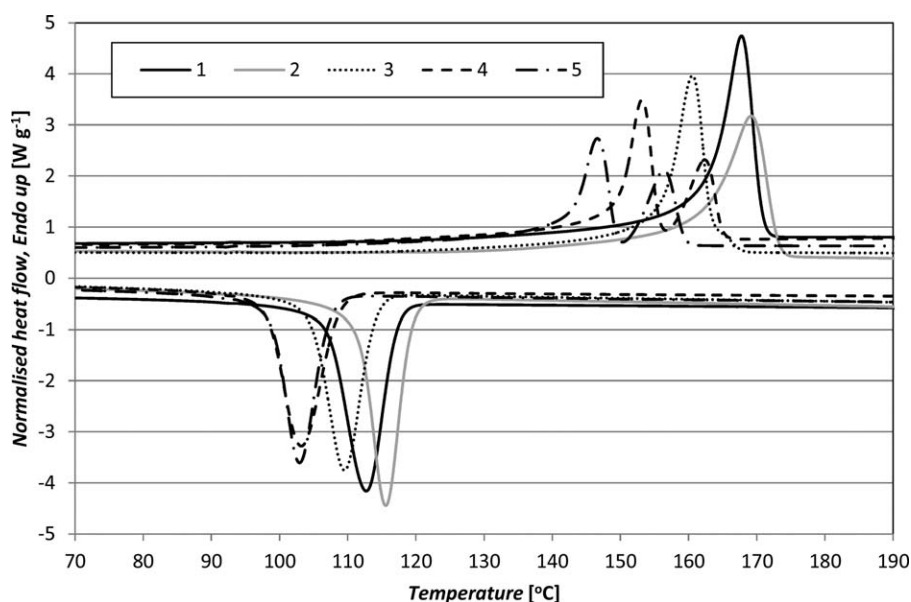


Figure 4. Melt endotherms (up) and crystallization exotherms (down) of (reactive) blended PHBV samples: 1—solid black (control); 2—solid grey (0% DCP); 3—dotted black (1% DCP); 4—dashed black (2% DCP); 5—dot/dashed black (4% DCP).

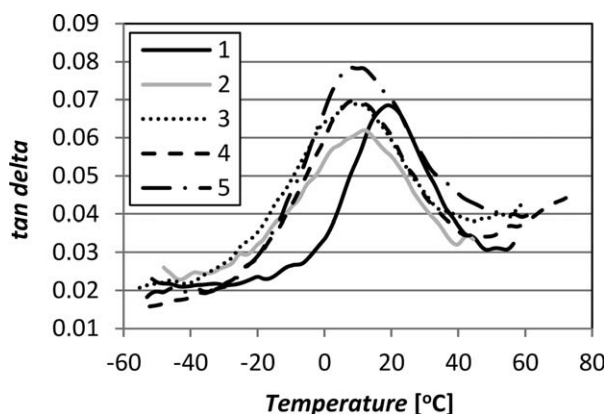


Figure 5. Glass transitions of PHBV by DMA (peak in $\tan \delta$) with and without reactive blending. 1—solid black (control); 2—solid grey (0% DCP); 3—dotted black (1% DCP); 4—dashed black (2% DCP); 5—dot/dashed black (4% DCP).

noted. First (and in agreement with the literature), T_m of the first melting peak was found to decrease as the concentration of DCP was increased, which suggests a similar increase in backbone modification (although this could not be quantified). Second (and in contrast with the literature), the T_m of the second melting peak in this study was also found to decrease, which might be interpreted to suggest a more permanent degree of chain immobilization resulting from cross-linking. The enthalpies of melting and crystallization were also found to decrease as DCP concentration was increased, consistent with a decrease in overall crystallinity of the materials. These data are considered to support successful modification of the PHBV backbone, most likely by cross-linking, but perhaps with a contribution from grafting.

T_g was then measured using both DSC and DMA (Table III) with the aim of distinguishing between types of reaction of the linalool with the PHBV. It was hypothesized that cross-linking would lead to an increase in T_g by constraining molecular motions, while incorporation of linalool as side groups could lead to either an increase or a decrease in T_g depending on the balance of the potential hindrance to molecular rotation and the increase in free volume. Measurement of the PHBV T_g using DSC can be difficult due to the high crystallinity of the polymer and its small change in heat capacity on going through T_g . In this case, using a fast heating rate of $100^\circ\text{C min}^{-1}$ magnified the T_g such that it could be observed, although the transition was still not particularly clear for sample 2 (see Supporting Information). The T_g became easier to distinguish as the concentration of DCP was increased due to a rise in the change in heat capacity of the material across the glass transition, probably arising from the lower crystallinity/higher amorphous content of the reactive blended samples. Measurement of T_g by DMA provided data where the DSC data were unclear, however, direct read-across between the two techniques is not possible due to the additional frequency dependence of DMA and the different heating rates used.

DMA showed the T_g of 2 to be lower than the control, as would be expected from the small linalool molecule acting as a plasticizer. Little change was observed in the T_g by DSC as low levels

of DCP initiator were added (3), but an increase in T_g was evident for samples 4 and 5, which could indicate cross-linking in these materials. This trend was not as clear in the DMA data, however, the change in the $\tan \delta$ T_g peak shape may provide additional insights (Figure 5). In particular, a low-temperature shoulder to the peak was present for samples 2 and 3, which disappeared in sample 4 and was replaced by a high-temperature tail for sample 5. These data, taken in correlation with other observations, may indicate a proportion of grafting/plasticization occurring at low DCP concentration with a shift to predominant cross-linking at high DCP concentration. Such a conclusion would be consistent with that reported by Fei *et al.*¹⁵

Physical Characterization and Aging

Tensile testing of the materials was carried out to determine the effect of grafting/cross-linking on ultimate tensile strength (UTS) and strain at break. PHBV is well known to be a brittle material and it was hoped that grafting or cross-linking could provide property improvements in these areas. The UTS showed a small increase as the concentration of DCP was increased (Figure 6). The trend in strain at break was unclear due to a much higher than expected increase for sample 3 relative to the other samples. The difference in sample 3 may be related to other factors such as storage conditions or age at test, so firm conclusions cannot be drawn. However, in general, reactive blending resulted in an increase in strain at break.

In addition to the time zero properties measured above, a short (3 month), ambient temperature aging study was initiated to look at changes in mechanical properties over time (such as embrittlement associated with secondary crystallization). The results of that study were clearest in the tensile strain data and are shown in Figure 7. Data were normalized to show the change in strain with time and enable comparison of results in the absence of differences in initial strain. In all samples, an initial decrease in strain at break was observed followed by a period of equilibration at 30–60 days. The behavior of sample 1 was consistent with that reported by Corre *et al.* for Enmat Y1000P in a similar experiment, showing an approximately 70% reduction in strain at break within 30 days.⁶ The change in strain at break was generally reduced for reactive blended

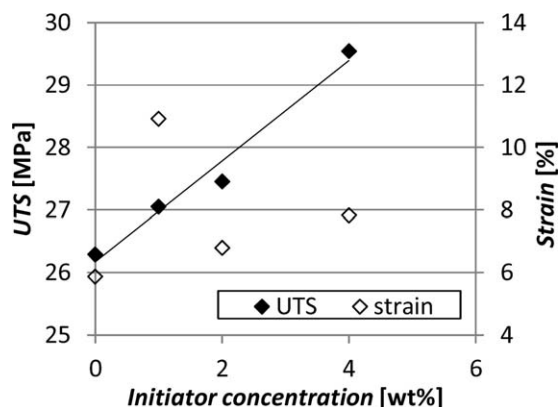


Figure 6. Initial tensile properties as a function of DCP content for samples 2–5 (solid line—break stress; dashed line—break strain).

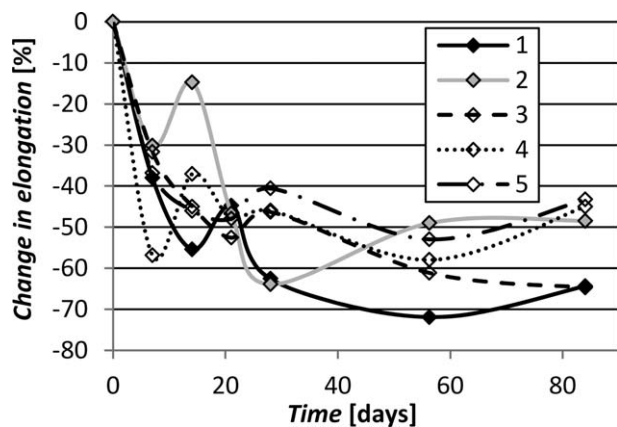


Figure 7. Influence of secondary crystallization on mechanical properties indicated by change in elongation at break over a 3 month ambient temperature ageing study. 1—black, solid; 2—grey, solid; 3—black, dashed; 4—black, dotted; 5—black, dot/dashed.

samples and especially for samples 4 and 5 with higher DCP concentrations as would be expected. These data indicate that reactive blending using natural monoterpene derivatives is a promising approach for the reduction of long-term embrittlement, but the system needs further optimization to find the correct level and combination of additives and further characterization to better understand the mechanism of the property changes.

CONCLUSIONS

Thermal and mechanical properties of PHBV were successfully modified with a one-step reactive blending approach using a free-radical initiator and biosourceable unsaturated modifier. The processing window of PHBV was broadened following this process due to a reduction in the melting temperature. Therefore, materials prepared in this way might be subsequently extruded at lower temperatures such that reduced thermal degradation would be expected to occur. The crystallization of the material was also reduced, resulting in an increase in elongation at break. The property modifications achieved extended to the longer term, with reduced embrittlement of reactive blended materials on ambient temperature aging. The chemical mechanism for the property changes could not be fully elucidated due to its complexity, but was thought to include a free-radical cross-linking component, mediated by the unsaturated modifier.

ACKNOWLEDGMENTS

The authors are grateful for the funding received from the European Union, FP7, project number 289521 (ISA-Pack). Specific thanks to John Gilling (Pera Technology) for assistance with polymer melt processing, David Corrigan (Pera Technology) for GC analysis, Frank Biddlestone (University of Birmingham) for assistance with DMA analysis, and Gerry Griffith (University of Leicester) for NMR analysis. Thanks also to colleagues in the ISA-Pack project who contributed with helpful discussions through the course of this investigation.

REFERENCES

- Chandra, R.; Rustgi, R. *Prog. Polym. Sci.* **1998**, *23*, 1273.
- Nair, L. S.; Laurencin, C. T. *Prog. Polym. Sci.* **2007**, *32*, 762.
- Puppi, D.; Chiellini, F.; Piras, A. M.; Chiellini, E. *Prog. Polym. Sci.* **2010**, *35*, 403.
- Reddy, M. M.; Vivekanandhan, S.; Misra, M.; Bhatia, S. K.; Mohanty, A. K. *Prog. Polym. Sci.* **2013**, *38*, 1653.
- Laycock, B.; Halley, P.; Pratt, S.; Werker, A.; Lant, P. *Prog. Polym. Sci.* **2013**, *38*, 536.
- Corre, Y.-M.; Bruzaud, S.; Audic, J.-L.; Grohens, Y. *Polym. Test.* **2012**, *31*, 226.
- Chen, G.-Q. *Chem. Soc. Rev.* **2009**, *38*, 2434.
- Sadik, T.; Massardier, V.; Becquart, F.; Taha, M. *Polymer* **2012**, *53*, 4585.
- El-Hadi, A.; Schnabel, R.; Straube, E.; Müller, G.; Henning, S. *Polym. Test.* **2002**, *21*, 665.
- An, Y.; Dong, L.; Xing, P.; Zhuang, Y.; Mo, Z.; Feng, Z. *Eur. Polym. J.* **1997**, *33*, 1449.
- Zhang, Q.; Zhang, Y.; Wang, F.; Liu, L.; Wang, C. *J. Mater. Sci. Tech.* **1998**, *14*, 95.
- Yoon, J.-S.; Lee, W.-S.; Jin, H.-J.; Chin, I.-J.; Kim, M.-N.; Go, J.-H. *Eur. Polym. J.* **1999**, *35*, 781.
- Yu, L.; Dean, K.; Li, L. *Prog. Polym. Sci.* **2006**, *31*, 576.
- Misra, M.; Desai, S. M.; Mohanty, A. K.; Drzal, L. T. *ANTEC Proceedings 2004 (Chicago, IL, USA)* **2004**, *2*, 2442.
- Fei, B.; Chen, C.; Chen, S.; Peng, S.; Zhuang, Y.; An, Y.; Dong, L. *Polym. Int.* **2004**, *53*, 937.
- Moad, G. *Prog. Polym. Sci.* **1999**, *24*, 81.
- Hassouna, F.; Raquez, J.-M.; Addiego, F.; Toniazco, V.; Dubois, P.; Ruch, D. *Eur. Polym. J.* **2012**, *48*, 404.
- Hassouna, F.; Raquez, J.-M.; Addiego, F.; Dubois, P.; Toniazco, V.; Ruch, D. *Eur. Polym. J.* **2011**, *47*, 2134.
- Leiner, J.; Stolle, A.; Ondruschka, B.; Netscher, T.; Bonrath, W. *Molecules* **2013**, *18*, 8358.
- Pathak, S.; Srivastava, A. K. *Des. Monom. Polym.* **2005**, *8*, 409.
- National Institute of Standards and Technology, NIST Chemistry WebBook. Available at: <http://webbook.nist.gov/chemistry/>, accessed on January 21, 2015.
- Fei, B.; Chen, C.; Wu, H.; Peng, S.; Wang, X.; Dong, L.; Xin, J. H. *Polymer* **2004**, *45*, 6275.
- O'Brien, N.; McKee, A.; Sherrington, D. C.; Slark, A. T.; Titterton, A. *Polymer* **2000**, *41*, 6027.
- Bannister, I.; Billingham, N. C.; Armes, S. P.; Rannard, S. P.; Findlay, P. *Macromolecules* **2006**, *39*, 7483.
- Chen, C.; Fei, B.; Peng, S.; Zhuang, Y.; Dong, L. *Eur. Polym. J.* **2002**, *38*, 1663.